Journal of Nuclear Materials 389 (2009) 78–84

Contents lists available at ScienceDirect

Journal of Nuclear Materials

journal homepage: www.elsevier.com/locate/jnucmat

Radial redistribution of actinides in irradiated FR-MOX fuels

Koji Maeda [a,*], Shinji Sasaki [a], Masato Kato [b], Yoshiyuki Kihara [b]

[a] *Oarai Research and Development Center, Japan Atomic Energy Agency, 4002 Narita, Oarai, Ibaraki 311-1393, Japan*
[b] *Nuclear Fuel Cycle Engineering Research Institute, Japan Atomic Energy Agency, 4-33 Muramatsu, Tokai-mura, Naka-gun, Ibaraki 319-1194, Japan*

ARTICLE INFO

PACS:
28.41.Bm

ABSTRACT

The redistributions of neptunium, plutonium and americium during two kinds of short-term irradiation tests for 10 min and 24 h at high linear heating rate around 430 W cm^{-1} were studied in the uranium and plutonium mixed oxide fuel containing Am and/or Np. It was found in the irradiation test for 24 h that the concentrations of Pu and Am increased toward the central void, but there was no change in the concentration of Np. The obtained experimental redistributions of Am and Pu were analyzed, based on both pore migration and thermal diffusion models. As a result, the calculated redistributions of Pu and Am showed good agreements with the experimentally obtained ones.

1. Introduction

A uranium (U) and plutonium (Pu) mixed oxide (MOX) fuel containing minor actinides (MA-MOX) is a promising candidate fuel not only to transmute long life MAs in fast breeder reactors (FBR), but to establish a FBR cycle with high potential of non-proliferation. Several studies were carried out on the thermal properties of these fuels, but the irradiation performance of the homogeneous MA-MOX fuel containing small amounts of MAs has been studied only in the SUPERFACT experiment [1]. Therefore, there are still only limited data regarding the irradiation behavior of the MA-MOX fuel.

Recently, the studies on the MA-MOX fuels containing americium (Am) up to 5 wt% and/or neptunium (Np) up to 12 wt% have been proceeding in Japan. These fuels have been fabricated by the conventional fuel fabrication method so as not to modify the present fuel cycle [2,3], and their thermal properties have been reported in several papers and proceedings. However, only a few of investigations on the irradiation performance have been done.

Radial redistribution of actinide nuclides in MA-MOX fuel during irradiation has significant effects on the thermal properties such as melting, thermal conductivity and so on. Thus, the knowledge on this redistribution is very important to the design and integrity of fuel pins. A number of studies on the Pu redistribution have been reported until now, but no study on the redistributions of actinide nuclides has been published.

In this study, two kinds of irradiation experiments were carried out to investigate the redistributions of actinide nuclides in MA-MOX fuels, which were fabricated by the conventional fabrication method. These results were quantitatively analyzed based on the pore migration and thermal diffusion models. The results obtained in two kinds of experiments were discussed and compared with the experimental results.

2. Experimental

Two kinds of fuel specimens used in this study were MOX fuels containing Np and Am (Np–Am-MOX) and MOX fuel containing less than 1% of Am (Am-MOX). The fuel pellets were fabricated from the powders co-converted by the microwave heating, based on the conventional method used in Japan. The diameter and density of pellets were nearly 5.42 mm and 93% of the theoretical density. In addition, the O/M ratios of both pellets were adjusted to 1.95 and 1.98. Other details of fuel pellets are shown in Table 1, together with the irradiation conditions described later.

These fuel pellets were inserted into three Joyo MK-III core fuel pins by substituting some of the conventional pellets in the axially central region (200 mm in length). The cladding of these fuel pins was made of PNC-316, and their outer diameter and thickness were nearly 6.5 and 0.47 mm, respectively.

Two types of irradiation tests, Am1-1 and Am1-2 were carried out. The kinds of pellets included in both irradiation tests and their maximum linear heating rate (LHR) and local burn-up are shown in Table 1. In this table, axial positions of fuel specimens are signified by x/L. Here, L equals the total length of inserted pellets and is 200 mm. x is the distance from the bottom of inserted pellets to the position. Axial positions of maximum linear heating rate and fuel temperature correspond to $x/L = 0.5$ (the rector core mid-plane) and 0.54, respectively.

The irradiation, Am1-2 followed the Am1-1 irradiation; irradiation histories are shown in Fig. 1. The maximum reactor power

---

[*] Corresponding author. Tel.: +81 29 267 4141; fax: +81 29 267 7130.
E-mail address: maeda.koji@jaea.go.jp (K. Maeda).

0022-3115/$ - see front matter © 2009 Elsevier B.V. All rights reserved.
doi:10.1016/j.jnucmat.2009.01.010

Table 1
Fuel specifications and irradiation conditions.

Irradiation test	Fuel pin ID	Fuel type	*x*/*L*	Fuel specification						Irradiation conditions	
				Am content (wt%)	Np content (wt%)	Fuel density (%TD)	O/M	Pu content (wt%)	Diameter (mm)	Linear heat rating (W/cm)	Local burnup (at%)
Am1-1 (10 min test)	Am1-1-1	Am-MOX	0.68	0.5	–	93	1.98	27.00	5.42	416	0.0072
		Np–Am-MOX	0.50	2.0				28.80		427	0.0082
Am1-2 (24 h test)	Am1-2-1	Am-MOX	0.26	0.5	–	93	1.98	27.00	5.42	424	0.0356
		Am-MOX	0.74							420	0.0361
		Np–Am-MOX	0.50	2.0	2.0			28.80		432	0.0369
		Np–Am-MOX	0.54							432	0.0370
	Am1-2-2	Am-MOX	0.26	0.5	–	93	1.98	27.00	5.42	421	0.0243
		Am-MOX	0.74							417	0.0247
		Np–Am-MOX	0.50	2.0	2.0			28.80		429	0.0256
		Np–Am-MOX	0.54							429	0.0256

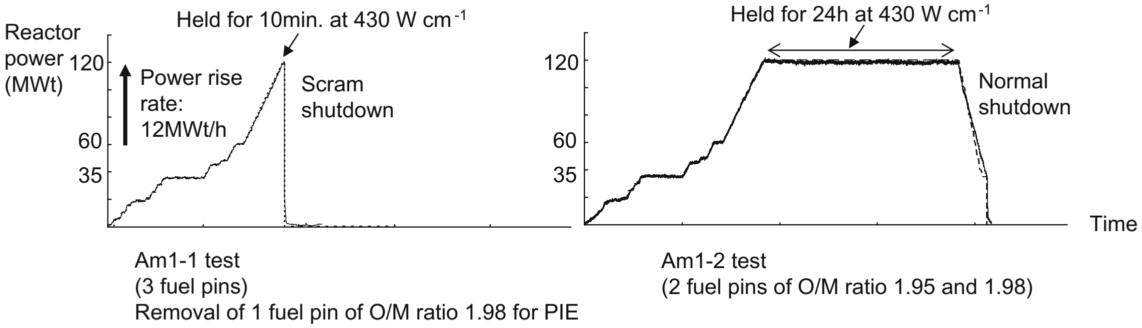

Fig. 1. The reactor power histories in two short-term irradiation tests.

level corresponds approximately to 430 W cm^{-1} of linear heating rate [4]. The fuel pellets were irradiated at the maximum LHR for only 10 min in Am1-1 and for 24 h in Am1-2. Further, Am1-2 was divided into two groups, Am1-2-1 and Am1-2-2, depending on the O/M ratios of fuel pellets.

After the irradiations, non-destructive post irradiation examinations (PIEs) of these irradiated fuel pins were carried by the same method as done in the conventional fuel pins. After confirming the integrities, these irradiated fuel pins were sectioned for the destructive PIEs. The fuel pin irradiated in Am1-1 was sectioned at two axial positions, while two fuel pins irradiated in Am1-2 were sectioned at 4 axial positions.

The obtained transverse sections were mirror-polished and were subjected to the destructive PIEs. The microstructures were observed by an optical microscope. The radial distributions of U, Np, Pu and Am were quantitatively measured with a shield electron probe micro analyzer (EPMA).

The following parameters were selected for the analysis: acceleration voltage, 20 kV; beam current for point analysis, 50 nA; using a PET diffracting crystal. U, Np and Am were analyzed with M_α characteristic X-ray line. Pu was analyzed with the line M_β line, and the intensity of the Pu M_β line was corrected by taking into consideration the overlap with the U M_β line. The concentration measured in non-irradiated MOX pellet containing 1% Am was used as the standard for the analyses of Am and Pu in the irradiated pellets. The concentration of Np in non-irradiated 2%Np-2%Am-MOX pellet was used as the standard for the analysis of Np in the irradiated Np-Am-MOX pellets.

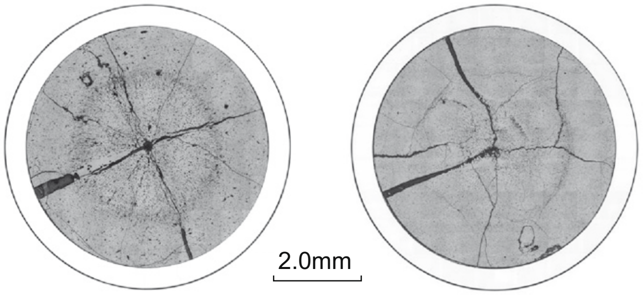

(a) x/L=0.50
Np-Am-MOX fuel

(b) x/L=0.68
Am-MOX fuel

Fig. 2. Ceramographs of specimens sectioned from the fuel pin irradiated in the Am-1-1 experiment.

3. Results

3.1. Microstructural observations

The microstructures of two kinds of fuel pellets irradiated in Am1-1 are shown in Fig. 2. No central void can be seen in either kind of fuel pellets. It is understood that the duration of irradiation at maximum LHR is too short to form the central void.

The microstructures of fuel pellets irradiated in Am1-2 are shown in Figs. 3a and b. The central voids can be seen in both groups of Am1-2 fuel pellets, but there is little difference among the void sizes in them. It has been reported in many papers that the decrease of O/M ratio decreases the thermal conductivity, but this effect of O/M ratio on fuel microstructure between both groups of fuel pellets is not observed. Comparison with specimens with O/M ratio = 1.98 at the reactor core mid-plane position shows fuel restructuring of Np–Am-MOX fuel began even in the Am1-1 test, and subsequently marked fuel restructuring accompanied by large central void formation is observed after the Am1-2 test.

3.2. Radial redistributions of Np, Pu and Am

All the ceramography specimens shown in Figs. 2 and 3 were also used for EPMA measurements for radial profiles of

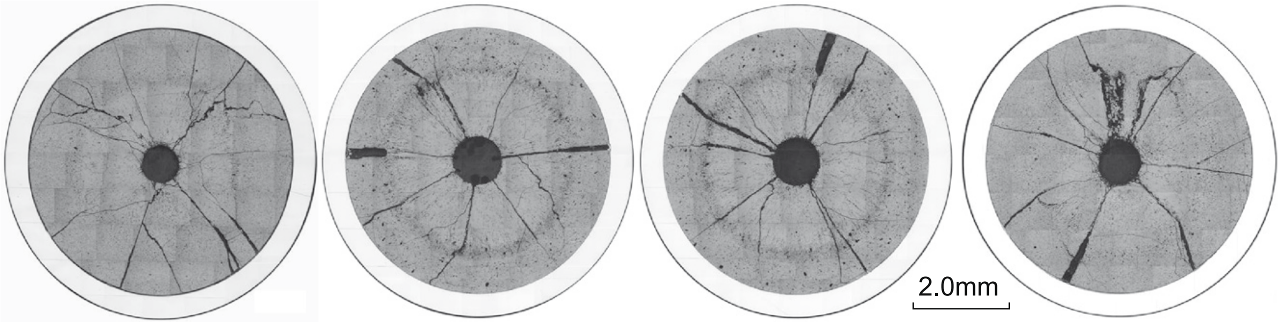

(a) x/L=0.26
Am-MOX fuel

(b) x/L=0.50
Np-Am-MOX fuel

(c) x/L=0.54
Np-Am-MOX fuel

(d) x/L=0.74
Am-MOX fuel

Fig. 3a. Ceramographs of specimens sectioned from the fuel pin of O/M ratio 1.98 irradiated in the Am1-2 experiment.

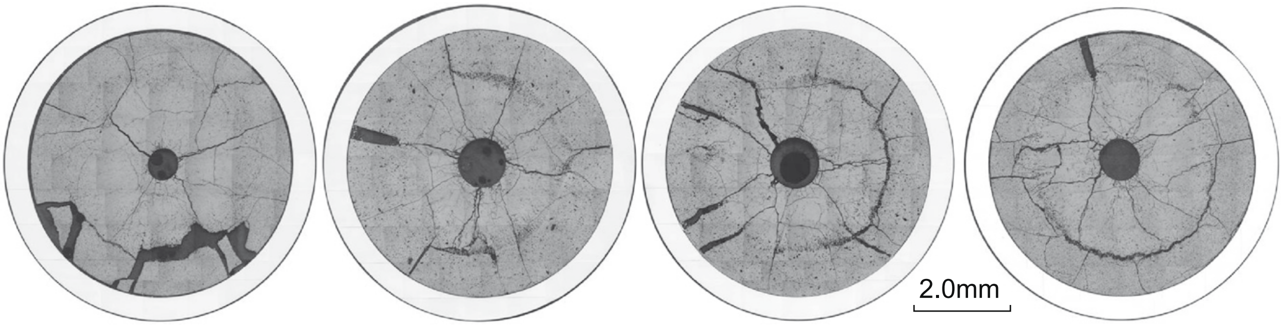

(a) x/L=0.26
Am-MOX fuel

(b) x/L=0.50
Np-Am-MOX fuel

(c) x/L=0.54
Np-Am-MOX fuel

(d) x/L=0.74
Am-MOX fuel

Fig. 3b. Ceramographs of specimens sectioned from the fuel pin of O/M ratio 1.95 irradiated in the Am1-2 experiment.

actinides. Quantitative data for all specimens are summarized in Table 2.

The radial distributions of Np, Pu and Am in the fuel pellets irradiated in Am1-1 are shown in Figs. 4a and b, but no significant change in the distributions is observed, because of too short duration of irradiation at the maximum LHR.

Figs. 5 and 6 show the radial distributions of Np, Pu and Am in both groups of fuel pellets irradiated in Am1-2. The concentrations of Pu and Am increase toward the central void, but the concentration of Np does not change with redial distance. It should be additionally noted that the degrees of increases of Pu and Am are larger in the fuel pellets having higher O/M ratio (=1.98) than in the ones having lower O/M ratio (=1.95). It can be understood that the basis of evaporation–condensation mechanism in migrating pores during fuel restructuring. Since the total vapor pressure over the solid is reduced as the O to M ratio decreases. The concentrations of three actinide elements decrease at the region around 0.8 mm from fuel surface. This is explained from the fact that this region corresponds to the boundary between the equiaxed and columnar grain structures and is rich in the voids.

Pu and Am concentrations near the central void of the fuels as a function of linear heating rate are shown in Fig. 7a. A comparison of the amount of Pu increase near the central void with the amount of Am increase is shown in Fig. 7b. Here, the amount of increase is defined as the difference before and after the irradiation. The radial profiles of Am and Pu are similar in specimens; however, the magnitude of Am increase near the central void is dependent on initial Am content.

4. Discussion

The redistributions of actinide elements in the MOX fuel under a steep temperature gradient have been studied by a number of researchers, and considered to be caused by the following two transport processes [5–12]: pore migration by evaporation and condensation, and thermal diffusion.

Assuming that the concentration, c for the expression of the redistribution is Pu/M or Am/M, the transport equation is generally given by the following equation.

$$\frac{\partial c}{\partial t} = -\frac{1}{r}\frac{\partial}{\partial r}\left[rJ_r\left(c, \frac{\partial c}{\partial r}, \frac{\partial^2 c}{\partial r^2}, r, t \right) \right] \tag{1}$$

Clement and Finnis [12] applied this equation to numerical analyses of Pu redistribution in MOX fuel in both cases of pore migration and thermal diffusion, and gave two solutions,

(1) Redistribution by pore migration:

$$\frac{c - c_0}{c} \approx \frac{P_0}{20}\frac{l}{d}\left|\frac{dT}{dr}\right|\frac{d\overline{D}}{dr}t\left(1 + \frac{1}{2}t\frac{dv}{dr}\right), \tag{2}$$

where T is temperature in K, and c_0 is initial concentration before irradiation. l and d are the pore diameter (80 μm) and thickness (8 μm), respectively, P_0 is the initial porosity, and $\overline{D}$ and E^* are a mean value for the Pu/U and Am/U diffusivity in the enhanced layer and the activation energy for the Pu–U, Am–U diffusivity,

Table 2
Summary of radial redistribution data of actinide obtained in the Am1-1 amd Am1-2 experiments.

Am1-1-1 pin

Np-Am-MOX (x/L=0.50, O/M 1.98)

Distance (mm)	Am(wt%)	Np(wt%)	Pu(wt%)	U(wt%)
0.00	2.00	2.11	26.79	69.10
0.25	1.84	1.00	25.21	71.95
0.50	2.25	2.01	29.75	65.99
0.70	1.69	2.05	25.36	70.90
0.90	1.95	1.98	26.97	69.10
1.10	1.49	2.17	23.49	72.85
1.30	1.44	2.19	22.80	73.58
1.50	1.80	1.94	26.52	69.74
1.70	2.06	2.11	28.72	67.11
1.90	2.13	2.10	28.45	67.32
2.10	2.21	1.96	28.44	67.38
2.30	2.15	2.08	28.49	67.27
2.50	2.15	1.68	27.79	68.37
2.65	2.30	1.97	28.00	67.73

Am-MOX (x/L=0.68, O/M 1.98)

Distance (mm)	Am(wt%)	Pu(wt%)	U(wt%)
0.00	0.60	24.05	75.35
0.50	0.42	24.14	75.44
0.85	0.53	24.97	74.50
1.00	0.41	23.14	76.44
1.10	0.45	24.73	74.82
1.55	0.58	25.78	73.65
1.90	0.57	24.56	74.87
2.10	0.54	25.63	73.83
2.35	0.64	25.75	73.62
2.40	0.54	26.94	72.53
2.45	0.54	25.96	73.50
2.55	0.62	25.56	73.82

Am1-2-1 pin

Am-MOX (x/L=0.26, O/M 1.98)

Distance (mm)	Am(wt%)	Pu(wt%)	U(wt%)
0.00	0.39	24.44	75.17
0.30	0.47	25.65	73.88
0.60	0.38	24.30	75.33
0.90	0.50	24.31	75.19
1.20	0.37	23.07	76.56
1.40	0.49	25.52	73.99
1.60	0.38	25.13	74.48
1.80	0.48	24.64	74.89
1.95	0.61	25.57	73.82
2.05	0.60	25.70	73.70
2.15	0.46	26.44	73.10
2.25	0.70	29.64	69.66
2.35	0.89	29.45	69.66

Np-Am-MOX (x/L=0.50, O/M 1.98)

Distance (mm)	Am(wt%)	Np(wt%)	Pu(wt%)	U(wt%)
0.00	1.93	2.37	26.35	69.35
0.30	2.32	1.91	28.65	67.12
0.60	1.83	1.65	25.46	71.05
0.80	1.42	1.95	23.90	72.73
1.00	1.70	1.89	25.00	71.41
1.20	1.89	2.02	26.38	69.71
1.40	2.23	1.92	28.16	67.69
1.60	2.30	2.06	28.63	67.01
1.70	2.13	1.86	27.25	68.77
1.80	2.27	1.80	26.68	69.24
1.90	2.13	1.92	28.69	67.26
2.00	2.13	2.04	28.78	67.06
2.05	2.40	1.84	29.45	66.31
2.10	2.61	1.88	30.11	65.39
2.15	2.69	1.85	31.43	64.04
2.20	3.12	2.00	32.90	61.98

Np-Am-MOX (x/L=0.54, O/M 1.98)

Distance (mm)	Am(wt%)	Np(wt%)	Pu(wt%)	U(wt%)
0.00	1.78	0.87	25.56	71.78
0.20	1.76	1.49	24.51	72.24
0.30	2.00	1.83	28.42	67.75
0.40	1.91	2.01	25.75	70.34
0.50	1.83	1.81	26.32	70.03
0.70	1.55	1.87	25.09	71.48
0.85	1.62	1.85	25.15	71.37
1.00	1.24	2.00	26.73	70.03
1.20	1.75	1.76	27.25	69.24
1.40	2.10	2.10	28.01	67.79
1.60	2.01	1.84	26.82	69.33
1.80	2.23	1.85	26.14	69.77
2.00	2.07	0.65	27.19	70.08
2.10	2.25	2.06	29.63	66.07
2.15	2.51	1.99	31.82	63.68
2.25	3.16	2.10	34.14	60.60

Am-MOX (x/L=0.74, O/M 1.98)

Distance (mm)	Am(wt%)	Pu(wt%)	U(wt%)
0.00	0.49	25.22	74.29
0.30	0.51	23.79	75.69
0.60	0.39	24.31	75.30
0.90	0.35	24.20	75.46
1.20	0.46	24.53	75.01
1.50	0.54	24.27	75.19
1.80	0.48	23.93	75.59
2.00	0.46	23.93	75.61
2.10	0.78	24.35	74.87
2.20	0.55	26.80	72.65
2.30	1.01	33.25	65.74

Am1-2-2 pin

Am-MOX (x/L=0.26, O/M 1.95)

Distance (mm)	Am(wt%)	Pu(wt%)	U(wt%)
0.00	0.43	24.93	74.64
0.40	0.47	24.15	75.38
0.60	0.45	23.69	75.86
0.90	0.57	24.40	75.03
1.20	0.42	23.90	75.68
1.50	0.49	25.59	73.92
1.80	0.41	25.07	74.52
2.00	0.51	24.54	74.95
2.10	0.54	25.12	74.34
2.20	0.47	24.73	74.79
2.30	0.64	25.28	74.08
2.35	0.53	25.83	73.64
2.40	0.68	27.69	71.63

Np-Am-MOX (x/L=0.50, O/M 1.95)

Distance (mm)	Am(wt%)	Np(wt%)	Pu(wt%)	U(wt%)
0.00	2.64	1.82	28.28	67.25
0.10	1.99	2.10	27.18	68.73
0.30	1.65	1.91	25.84	70.60
0.50	2.05	2.28	26.50	69.18
0.75	1.33	1.52	21.73	75.42
1.00	1.86	1.62	26.85	69.67
1.20	2.00	1.91	28.46	67.63
1.50	2.08	1.96	27.78	68.18
1.75	1.95	1.95	27.28	68.82
1.90	1.86	1.84	27.07	69.23
2.00	2.05	1.74	26.90	69.31
2.10	2.11	1.90	28.01	67.98
2.20	2.62	1.98	29.79	65.60

Np-Am-MOX (x/L=0.54, O/M 1.95)

Distance (mm)	Am(wt%)	Np(wt%)	Pu(wt%)	U(wt%)
0.00	1.78	0.87	26.47	70.87
0.30	1.71	1.83	24.88	71.58
0.60	1.91	1.87	26.78	69.44
0.80	1.70	1.77	23.69	72.84
1.00	1.77	2.00	24.34	71.89
1.20	2.20	1.76	27.51	68.53
1.50	1.96	2.11	25.74	70.19
1.70	1.84	1.97	27.32	68.87
1.80	1.92	1.85	27.02	69.21
1.90	2.00	1.98	26.91	69.10
2.00	1.87	0.65	26.64	70.83
2.05	1.94	1.94	26.84	69.28
2.10	2.15	2.06	29.05	66.74
2.15	2.37	1.99	30.60	65.03
2.20	2.88	2.09	32.86	62.17

Am-MOX (x/L=0.74, O/M 1.95)

Distance (mm)	Am(wt%)	Pu(wt%)	U(wt%)
0.00	0.41	24.43	75.16
0.30	0.41	24.09	75.51
0.40	0.38	24.97	74.65
0.50	0.47	23.63	75.90
0.60	0.50	23.72	75.78
0.70	0.42	24.65	74.93
0.80	0.56	23.62	75.83
0.90	0.44	25.52	74.04
1.20	0.50	24.00	75.50
1.50	0.47	24.89	74.64
1.80	0.49	24.13	75.38
2.00	0.40	24.90	74.70
2.10	0.58	28.00	71.41
2.15	0.55	31.01	68.44
2.20	0.98	35.24	63.78

respectively. v is pore migration velocity and is given by Eq. (3) [13].

$$v = \frac{k p_0 \exp(-H/RT)}{P T^{3/2}} |dT/dr| \tag{3}$$

$$\begin{aligned}\ln[p_0 \exp(-H/RT)] = {} & -212.275 + 65.842(O/M) \\ & + 8.9453 \times 10^{-2} T \\ & - 2.55399 \times 10^{-2} (O/M) T + 2.9560 (O/M)^2 \\ & - 5.6541 \times 10^{-6} T^2 \end{aligned} \tag{4}$$

In addition, $\overline{D}$ is expressed as follow,

$$\frac{\overline{D}}{v} = \frac{D_0}{4220 l |dT/dr|} \exp\left[\left(66490 - \frac{E^*}{R}\right)/T\right] \tag{5}$$

(2) Redistribution by thermal diffusion:

$$\frac{c - c_0}{c} = (1 - c_0) D U t \tag{6}$$

where, with R as the gas constant,

$$D = D_0 \exp(-E^*/RT) \tag{7}$$

$$U = \frac{Q^*}{RT}\left[\left(\frac{E^*}{RT} - 2\right)\left(\frac{\nabla^2 T}{T}\right)^2 + \frac{\nabla^2 T}{T}\right] \tag{8}$$

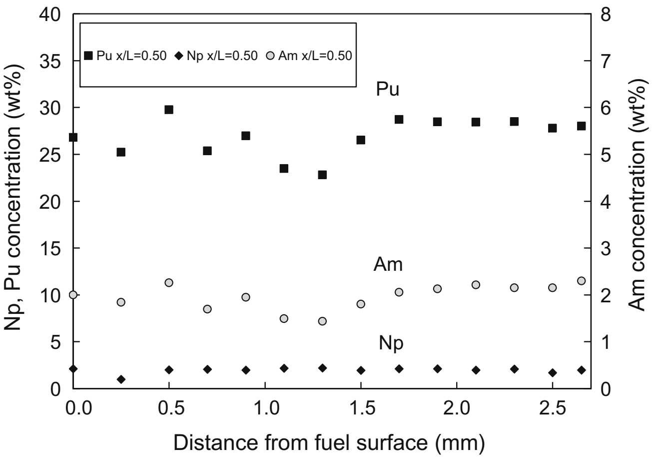

Fig. 4a. The radial profiles of Am, Np and Pu for the Np–Am-MOX fuel used in Am1-1 test.

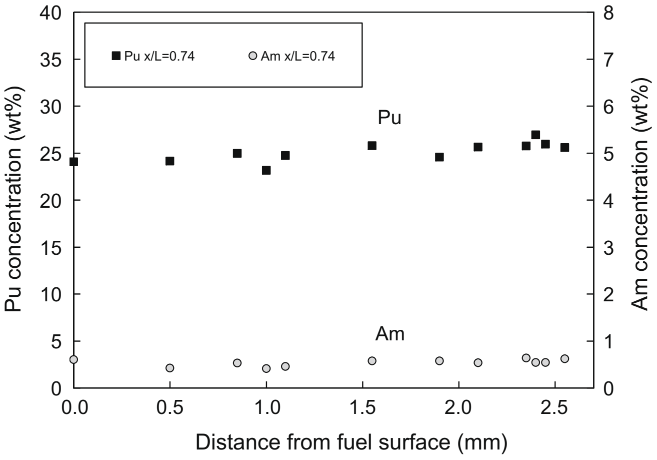

Fig. 4b. The radial profiles of Am and Pu for the Am-MOX fuel used in Am1-1 test.

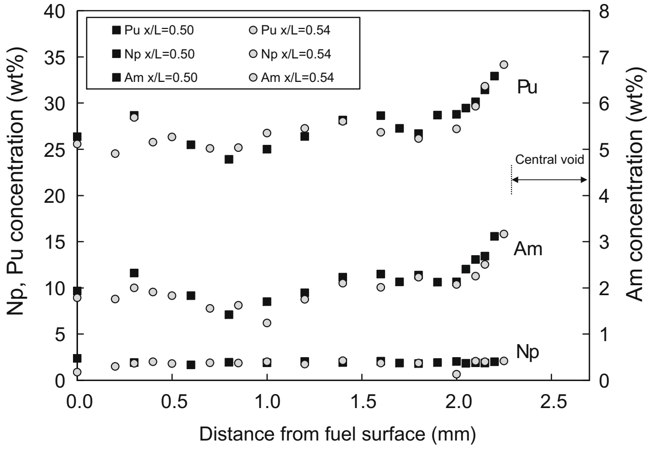

Fig. 5a. The radial profiles of Am, Np and Pu for the Np–Am-MOX fuel used in the Am1-2 test.

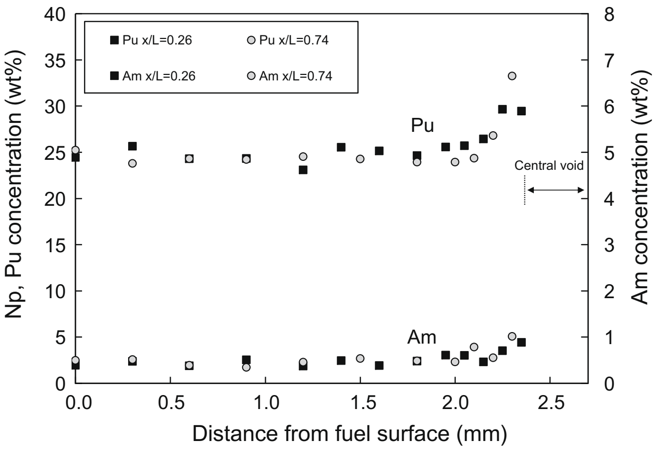

Fig. 5b. The radial profiles of Am and Pu for the Am-MOX fuel used in the Am1-2 test.

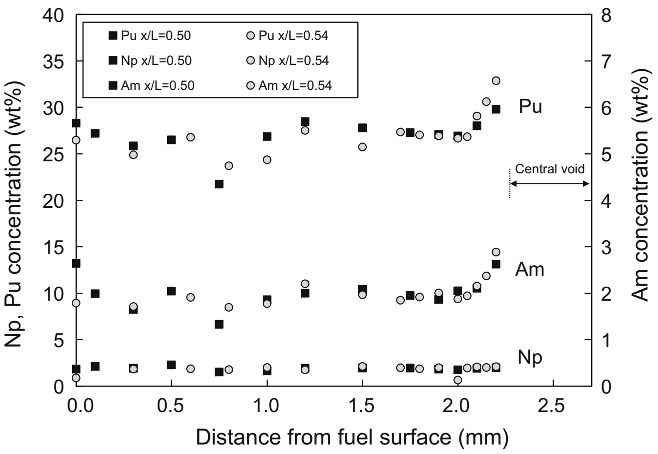

Fig. 6a. The radial profiles of Am, Np and Pu for the Np–Am-MOX fuel used in the Am1-2 test.

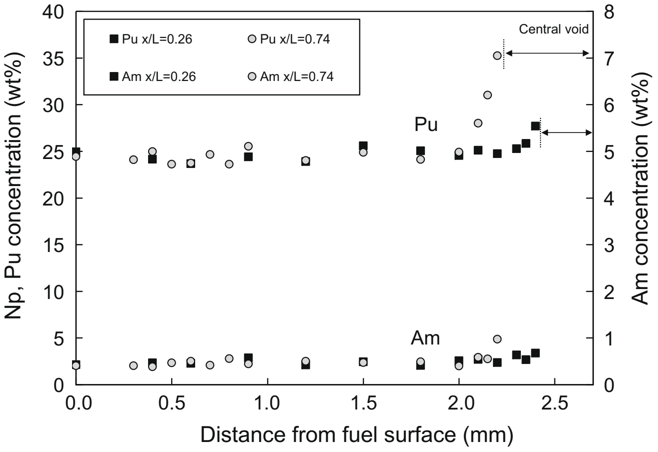

Fig. 6b. The radial profiles of Am, Np and Pu for the Np–Am-MOX fuel used in the Am1-2 test.

There have been a number of studies so far on the diffusion of U and Pu in UO_2 and MOX fuels. As the activation energy of diffusion, Bober and Schumacher used the values for $Q^* = -35$ kcal/mol, $E^* = 97.3$ kcal/mol and $D_0 = 0.34\ \text{cm}^2/\text{s}$ in their calculation of Pu redistribution [5], and Clement and Finnis applied $E^* = 105$ kcal/mol to their calculation [12]. In this study, the Pu redistributions were calculated by both values. As described later, a good result

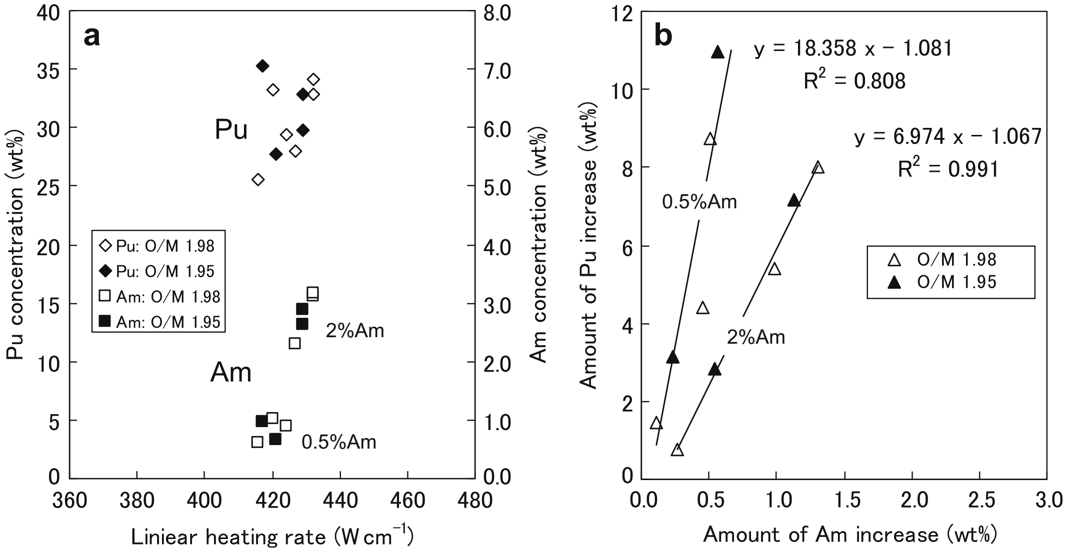

Fig. 7. (a) Pu and Am concentration near the central void as a function of linear heating rate and (b) comparison of the amounts of Pu and Am increase near the central void.

could be obtained by using $E^* = 107$ kcal/mol for fuel with O/M = 1.98. There has been only one paper on the diffusion of Am in UO_2 fuel, and the diffusion functions shown in that paper was used $D_0 = 0.02$ cm^2/sec and $E^* = 92$ kcal/mol for fuel with O/M = 1.98 in this study [14].

The temperature distribution in the fuel matrix was calculated by a conventional heat conduction equation of a cylindrical body. The temperature gradient obtained at the time intermediate between the beginning and end of irradiations was used in the analysis.

Based on the above assumptions, the redistributions of Pu and Am were calculated in the fuel pellets irradiated in Am1-1 by using both pore migration and thermal diffusion models. But the duration of irradiation was too short to find any detectable changes.

Next, the redistributions of Pu and Am were calculated in the fuel pellets irradiated in Am1-2 based on the pore migration model. Figs. 8a and b show the calculated results on for redistribution of Am and Pu irradiated in Am1-2, together with experimental results. The value of $E^*_{Pu} = 107$ and $E^*_{Am} = 92$ kcal/mol were used for the specimens of Am1-2-1 pin (O/M ratio = 1.98). The experimentally obtained redistributions of Pu and Am showed good agreement with the calculated ones.

Finally, calculations on the redistribution of Pu and Am were attempted in the fuel pellets irradiated in Am1-2 based on the thermal diffusion model. No significant redistribution could be found, since the duration of irradiation, 24 h was too short to cause any detectable redistribution by the thermal diffusion. Generally, the distance detectably affected by the diffusion is nearly $4\sqrt{Dt}$ [15]. Assuming that $D = 1.0 \times 10^{-10}$ cm^2/s at 2,400 K and $t = 86400$ s, then $4\sqrt{Dt}$ was about 0.1 mm. Also from this estimation, little significant change was expected in the redistribution.

As already shown in Figs. 5 and 6, the concentrations of Pu and Am increased with the increase of distance from the fuel surface. This was explained by considering the partial pressures of gaseous species in the lenticular pore. The partial pressures and compositions of U-bearing, Pu-bearing and Am-bearing gas species as a function of O/M ratio at 1800 and 2000 °C are shown in Figs. 9a and b, respectively, which were calculated from the formation energies of these oxides in the gaseous states, oxygen potential and vapor pressures, similarly to the references [16–18]. In Fig. 9, UO_3 is principal vapor species in the Am-MOX fuel when O/M ratio is over 1.96. Thus, UO_3 vapor was transported from the hotter to cool sides of lenticular pores, resulting in the enrichment of Pu

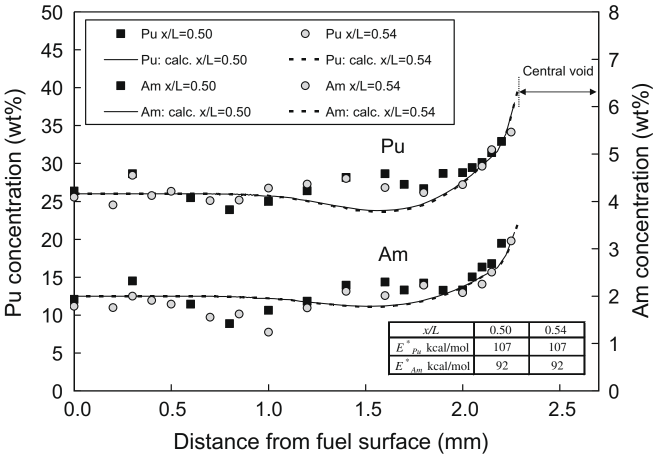

Fig. 8a. The radial profiles of Am and Pu for the Np–Am-MOX fuel used in the Am1-2 test (Am1-2-1 fuel pin, O/M = 1.98).

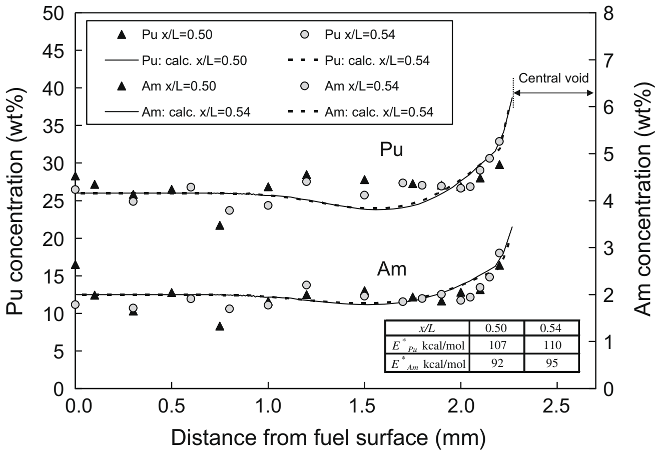

Fig. 8b. The radial profiles of Am and Pu for the Np–Am-MOX fuel used in the Am1-2 test (Am1-2-2 fuel pin, O/M = 1.95).

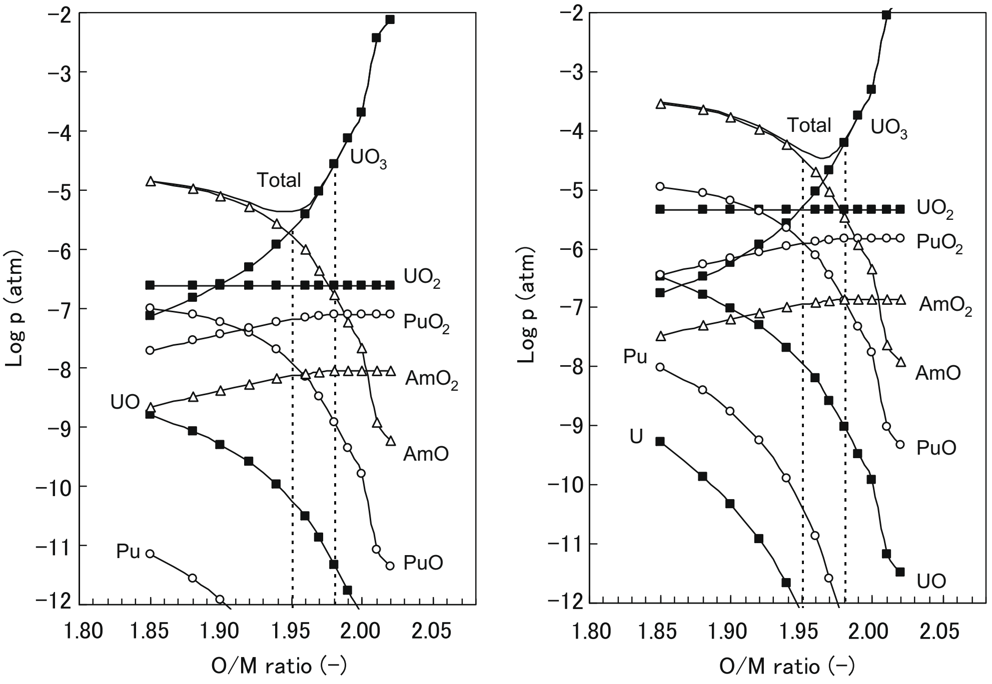

(a) 2%Am-MOX, 1800 ℃ (b) 2%Am-MOX, 2000 ℃

Fig. 9. The vapor pressure of U-bearing, Pu-bearing and Am-bearing gas species at temperatures of 1800 and 2000 °C.

and Am in the higher temperature region. On decreasing the O/M ratio below 1.96, the partial pressure of AmO is higher than that of UO_3, and it was expected that Am would become rich in the low temperature region, contradicting with the experimental result.

As a reason for this conflict, it was suggested that the content of Am was so small that the supply from the solid phase to the gas phase was too small to establish the equilibrium partial pressure shown in Fig. 9b. Then, UO_3 species was predominant in the gas phase of the lenticular pore also when O/M ratio was below 1.96. As already described, the extent of the redistribution was larger in fuel having initial O/M of 1.98 than in fuel having initial O/M of 1.95. This difference could be also understood from the above reason. That is, the partial pressure of UO_3 was higher in the fuel having initial O/M ratio of 1.98 than in the fuel having initial O/M ratio of 1.95.

5. Conclusions

MA-MOX fuels were prepared by the conventional fabrication method, and were irradiated in the experimental fast reactor, Joyo for 10 min and 24 h at high linear hating rate around 430 Wcm^{-1}. The redistributions of Np, Pu and Am were investigated in these fuels by the EPMA technique. The concentrations of Pu and Am increased with the increase of radial distance from the fuel surface, but no change was observed in the concentration of Np. In addition, the extent of redistribution was larger in the fuel of O/M = 1.98 than in the one of O/M = 1.95.

The obtained experimental redistributions were quantitatively analyzed, based on both pore migration and thermal diffusion models developed by Clement and Finnis. The redistributions analyzed based on the pore migration model showed good agreements with the experimental results. The difference in the extents of redistribution between the fuels of different O/M ratios was explained by considering the partial pressures of U, Pu and Am oxides in the gas phase of lenticular pore migrating toward the radial center of the fuel pellets.

Acknowledgements

The authors gratefully acknowledge very helpful discussions with Dr Hirotaka Furuya (Professor Emeritus, Kyusyu University). The authors also wish to gratefully acknowledge the contributions of Y. Ohsato, Y. Onuma, and S. Nukaga (Nuclear Technology and Engineering Corporation) for conducting the destructive PIEs.

References

[1] C.T. Walker, G. Nicolaou, J. Nucl. Mater. 218 (1995) 129.
[2] C. Prunier, F. Boussard, L. Kock, M. Coquerelle, in: Proceedings of GLOBAL ‘93, Seattle, Washington, USA, September 12–17, 1993.
[3] M. Ichimiya, T. Mizuno, M. Konomura, in: Proceedings of GLOBAL 2003, New Orleans, Louisiana, USA, November 16–20, 2003 (on cd-rom).
[4] T. Sekine, T. Soga, D.W. Wootan, S. Koyama, T. Aoyama, in: Proceedings of GLOBAL 2007, Boise, Idaho, USA, September 9–13, 2007 (on cd-rom).
[5] M. Bober, G. Schumacher, Adv. Nucl. Sci. Technol. 7 (1973) 21.
[6] M. Bober, G. Schumacher, D. Geithoff, J. Nucl. Mater. 47 (1973) 187.
[7] D.R. Olander, J. Nucl. Mater. 49 (1973/1974) 21.
[8] D.R. Olander, J. Nucl. Mater. 49 (1973/1974) 35.
[9] S. Guarro, D.R. Olander, J. Nucl. Mater. 57 (1975) 136.
[10] R.O. Meyer, D.R. O’Boyle, E.M. Butler, J. Nucl. Mater. 47 (1973) 265.
[11] R.O. Meyer, J. Nucl. Mater. 50 (1974) 11.
[12] C.F. Clement, M.W. Finnis, J. Nucl. Mater. 75 (1978) 193.
[13] W.J. Lackey, F.J. Homan, A.R. Olsen, Nucl. Technol. 16 (1972) 120.
[14] F. Schmitz, R. Lindner, J. Nucl. Mater. 17 (1965) 259.
[15] P.G. Shewmon, Diffusion in Solids, McGraw-Hill, 1963. p. 6.
[16] M.H. Rand, T.L. Markin, in: Thermodynamics of Nuclear Materials 1967, Proceedings of the IAEA Symposium, Vienna, 1968, p. 637.
[17] R.J. Ackermann, R.L. Faircloth, M.H. Rand, J. Chem. Phys. 70 (1966) 3698.
[18] H. Bailly, D. Menessier, C. Prunier, The nuclear fuels of pressurized and water reactors and fast reactors design and behaviour, Intercept Ltd., 1999, p.106.